

Copyright 2010, ABRACO

Trabalho apresentado durante o INTERCORR 2010, em Fortaleza/CE no mês de maio de 2010.

As informações e opiniões contidas neste trabalho são de exclusiva responsabilidade do(s) autor(es).

Comparative study of Ferritic Stainless Steels applied at High Temperatures

Moreto, J. A^{1*}, Gamboni, O. C², Ponte, H. A³, Moya, L. M⁴, Bueno, L. O⁵, S. Fofano⁶.

Abstract

The oil refineries in Brazil now face a huge challenge: to adapt their units for the processing of more aggressive petroleum in more critical conditions of pressure and temperature. One way to overcome these challenges is the use of new materials developed for such conditions. However, the lack of information about the behavior of these materials, when in operation for a long time cause uncertainty about the real performance of the same. This work presents a survey of the ferritic stainless steel tubes used in environments exposed to oxidation at high temperatures. The methodology for material selection used in these conditions was developed. Mechanical properties and phase transformations of ferritic stainless steel tubes (446 and kanthal alloy), used in radiation furnaces at Petrobras' schist processing plant, were evaluated. Hot tensile measures (ASTM E-21) and fluency (ASTM - E 139) were carried out on the materials sent to tests at different speeds and temperature. The method used for fluency data extrapolation was the Larson – Miller model (LM). Samples of tubes were analyzed by optical microscopy, scanning electron microscopy and energy dispersive spectroscopy.

Key-words: Ferritic stainless steel, hot tensile, creep, corrosion at high temperature.

Introduction

Tensile properties of metallic materials tested at high temperatures are, in general, affected by the strain rate ^[1]. Thus, controlling the specification of rates employed in testing is important. Standard ASTM E – 21^[2] specifies that in the beginning of the test and during creep, strain rate should be $0.005 \pm 0.002 \text{ min}^{-1}$, increasing to $0.05 \pm 0.01 \text{ min}^{-1}$ after the creep begins. However, depending on the sensitivity presented by the material's resistance to temperature and strain rate, the mere observance of these recommendations could lead to a quite limited assessment of the material performance ^[3]. When performing hot tensile testing of solid materials, using machines that develop constant strain rate on the specimen, different behaviors can be observed. The first is the strain hardening phenomenon that corresponds to the resistance increase caused by the deformation introduced to the test specimen. The second is the tensile strength phenomenon with the strain rate that represents resistance increase as the material is deformed at gradually higher strain rates.

One of the critical factors determining the integrity of components undergoing service at elevated temperatures is creep behavior. The creep phenomenon consists of the slow and

¹ Mestre, Engenheiro de Materiais – USP

² Químico – USP

³ Doutor, Engenheiro de Materiais – UFPR

⁴ Mestre, Engenheira de Materiais – UTFPR

⁵ PhD, Engenheiro de Materiais - UFSCar

⁶ Mestre, Engenheiro de Materiais - Petrobrás

progressive deformation accumulated over time, appearing in all crystalline solids under favorable temperature and stress conditions ^[4]. Theoretically, these phenomena can happen at any temperature above absolute zero to any metallic material, at a broad range comprising all the solid state. However, in most cases, the technological interest is limited to the homologous temperatures ($T_h = 0.5 T_f$) in the interval between 0.3 and 0.8 of the melting temperature of the base metal ^[4, 5]. Creep testing was carried out according to standard ASTM – E 139 ^[6], in the constant load modality.

Materials and Methods

Materials used in the present study were stainless steel A268/Tp 446 and powder metallurgy FeCrAl alloy APM by Kanthal alloy. These materials are normally used in high temperature furnaces and have application in steam generation systems of the chemical and petrochemical industries. The tube samples used in this study had dimensions: A268/Tp 446, length = 400 mm, $D_{ext} = 88.9$ mm, wall thickness = 4.5 mm; APM length = 400 mm, $D_{ext} = 88.9$ mm, wall thickness = 6.3 mm. Table 1 presents the chemical composition of A268/Tp 446 alloy.

Table 1 – Chemical composition of stainless steel A268/Tp 446 alloy

Chemical composition of A268/Tp 446 alloy	
Element	Composition (%)
Carbon	0,20
Manganese	1,50
Phosphorus	0,04
Sulfur	0,03
Silicon	1,0
Nickel	0,75
Chrome	23 – 27
Nitrogen	0,25

Table 2 presents the chemical composition of powder metallurgy FeCrAl alloy APM by kanthal alloy.

Table 2 – Chemical composition of APM alloy

Chemical composition of APM Alloy	
Element	Composition (%)
Carbon	0,08
Silicon	0,7
Manganese	0,4
Chrome	23,5
Aluminum	-
Iron	-

For hot tensile testing a Time Group universal testing machine model WDW – 100 with a 10 ton capacity was used. Testing was developed according to the recommendations of standard ASTM E – 21 ^[2] employing cylindrical body tests with threads in the heads as illustrated in Figure 1.

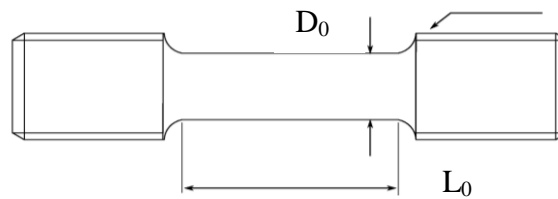


Figure 1 - Shape of Test Bodies Used in Hot Tensile Testing.

Specimens were longitudinally extracted from the tubing, with nominal size of: A268/Tp 446: gage - $L_0 \approx 12$ mm, $D_0 \approx 3.0$ mm and threaded heads - M 4 x 0,7; APM/ alloy: gage - $L_0 \approx 14$ mm, $D_0 \approx 3.5$ mm and thread heads - M 5 x 0,8.

The hot tensile testing was performed using an electric furnace of 2 KW of power with 3 heating zones built with alloy A1 resistance wire, together with temperature controllers of the Proportional-Integral-Differential (P-I-D) type, micro-processed. Temperature measurements were made by Chromel - Alumel (type K) thermocouples for $T < 700$ °C and (type S) Pt - 10% Pt-Rh for ≥ 700 °C.

A series of two tests was performed for each material at 6 temperatures (500°, 600°, 700°, 800°, 900° and 1000°C). Stress values ranged between 7.6 and 309.0 MPa. At each testing temperature one strain rate recommended by standard ASTM - E 21 of 0.01 min^{-1} ($1\% \text{ min}^{-1}$) was used. Twelve hot tensile tests were performed for each alloy. Figure 2a presents the equipment used in hot tensile testing.

Creep testing was of the single rupture type and was carried out in cylindrical specimens longitudinally extracted from tubing in the constant load modality in STM equipment, model MF-1000, following recommendations of the standard ASTM E - 139. Information about this equipment and testing techniques can be found in previous publications ^[7, 8]. Figure 2 shows the equipment used in hot tensile testing and creep testing.

Twenty-eight tests were made - 14 for each of the 2 alloys. Creep testing was performed at 9 temperature levels namely (550°, 600°, 625°, 650°, 700°, 750°, 800°C, 900° and 1000 °C), comprising stress values in the range between 10 and 125 MPa. Shapes and sizes of the specimens used in creep testing were similar to those used in tensile testing.



Figure 2 – Equipment used in this study: a) universal machine used in hot tensile testing and b) row of 10 machines used in creep testing.

Each specimen received puncture marks in the extremities of the operational part to define length L_0 , before testing. After conclusion of each test, fractured parts of the test bodies were united to measure final length L_f and final diameter d_f in the region of fracture, with the purpose of determining the final elongation percentage. Temperature measurements were made with type K and type S thermocouples. Creep data were treated with the Larson – Miller method. This method considers iso-stress lines converging to a point in the axis of ordinates, and is based on the parameter given by the expression:

$$T(C + \log t_r) = P \quad (1)$$

with C been the constant characteristic of the material. The C value is obtained through some tests at the same stress and different temperatures. For low alloy stainless steels, the C value is approximately 20^[9].

Results and Discussion

Figure 3a shows the nominal stress curve *versus* nominal strain of sample A268/Tp 446 tested at 600 °C with a strain rate of 0.01 mm/min that corresponds to a nominal strain rate of $1.282 \times 10^{-5} \text{ s}^{-1}$. The nominal strain rate (de/dt) was determined by the expression $de/dt = V_T/L_0$, where V_T is the tensile strain rate and L_0 is the initial length of the operational part of the specimen. It can be verified that the tensile strength is approximately 90.8 MPa and final rupture elongation of 109%. The tensile strength was determined at the maximum point of the stress curve *versus* strain. Figure 3b illustrates the initial part expanded to determine yield strength ($\sigma_{0.2}$). The value found was approximately 73.5 MPa.

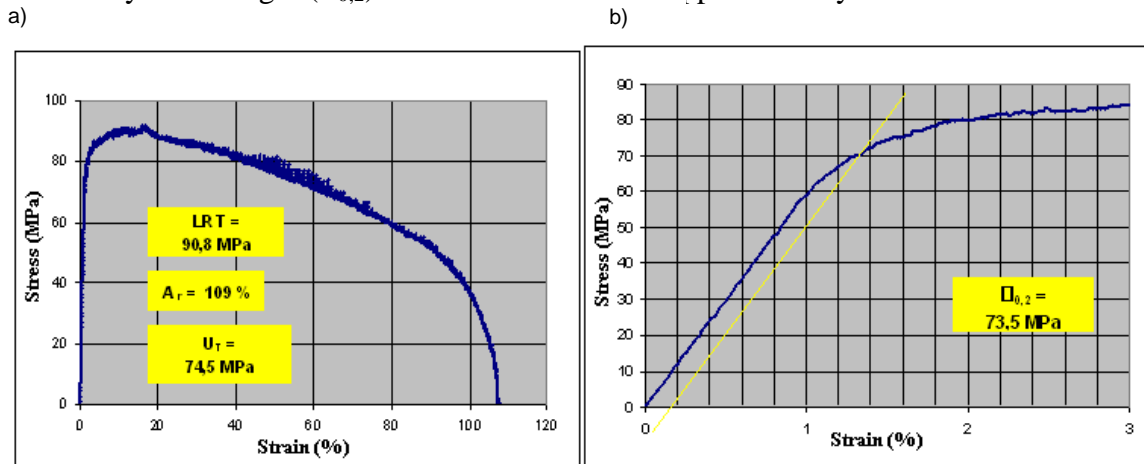


Figure 3 – a) Nominal Stress Curve vs. Nominal Sample Strain A268/Tp 446 Tested at 600°C, With $V_T = 0.01$ mm/min and b) Initial Part Expanded to Determine Yield Strength ($\sigma_{0.2}$).

In an analogous way, the specimen tested at 600 °C with strain rates of 0.12, 5 and 20 mm/min were analyzed. Figure 4a presents nominal stress curves *versus* nominal strain of sample A268/Tp 446 tested at 600 °C with velocities 0.01, 0.12, 5 and 20 mm/min.

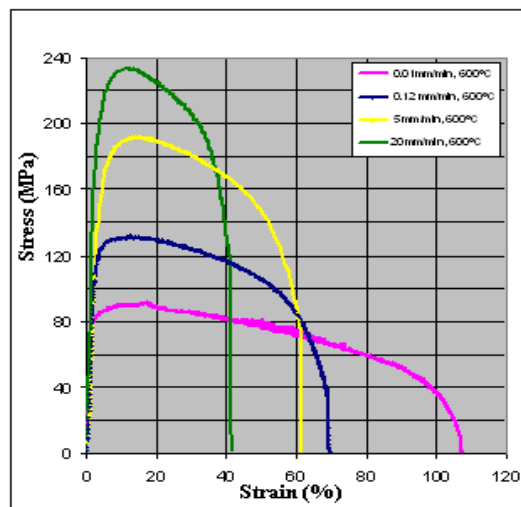


Figure 4a – curve reuniting results of hot tensile testing at temperature of 600°C for sample A268/Tp 446, With $V_T = 0.01, 0.12, 5$ and 20 Mm/Min.

The alloys showed a significant increase in tensile strength values and $\sigma_{0.2}$ with strain rate. Such an increase is due to strain rate sensitivity. All samples showed a chisel-type rupture, making determination of area reduction parameter (R.A.) indefinite. Table 3 presents results determined according to standard ASTM – E 21, of hot tensile testing performed at a 600 °C temperature for sample A268/Tp 446.

Table 3 – Data regarding hot tensile test for sample A 268/Tp 446.

Material A268 / Tp 446 / 600 °C					
CP	LRT (MPa)	$\sigma_{0.2}$ (MPa)	A_r in 4D (%)	R.A. (%)	Toughness (MPa)
A268 – $V_T = 0.01$ mm/min	90.8	73.5	109	*	74.5
A268 – $V_T = 0.12$ mm/min	132.5	109.0	70	*	75.4
A268 – $V_T = 5$ mm/min	191.9	142.0	62	*	988
A268 – $V_T = 20$ mm/min	233.1	147.1	41.4	*	83.4

By comparing the four curves in Figure 4b it is possible to verify that a variation in the tensile strain rate led to a change in strength and altering the nominal stress curve *versus* nominal strain. The alloy had strain rate sensitivity, showing higher resistance levels at higher tensile strain rate. According to Table 4 it is possible to verify that the higher the tensile strain rate, the smaller the size variation of the specimen.

Figure 4b shows the nominal stress curve *versus* nominal strain of alloy APM tested at strain rates 0.01, 0.14, 5 and 20 mm/min at 600 °C. Table 4 presents the results, determined according to standard ASTM E – 21 of elevated temperature tensile testing at 600 °C at different strain rates for this alloy.

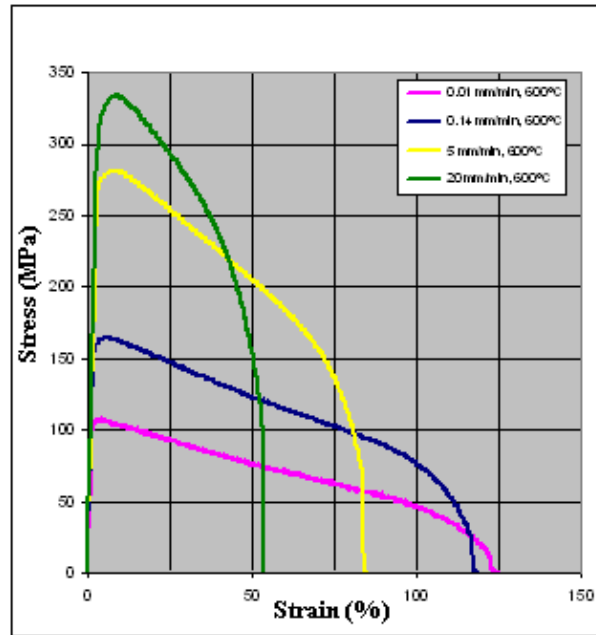


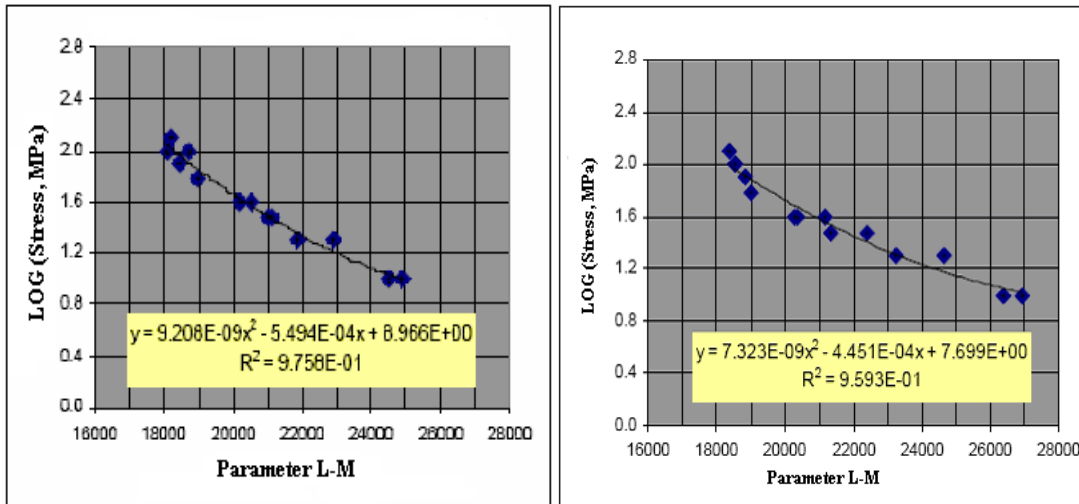
Figure 4b - Nominal stress curves vs. nominal strain for alloy APM tested at strain rates of 0.01, 0.14 and 5 mm/min at temperature of 600°C.

Table 4 – Data regarding hot tensile test for sample APM alloy.

Material APM / 600 °C					
CP	LRT (MPa)	$\sigma_{0,2}$ (MPa)	A_r in 4D (%)	R.A. (%)	Toughness (MPa)
APM – $V_T = 0,01$ mm/min	108.5	103.7	123	*	59.6
APM – $V_T = 0,14$ mm/min	164.9	160.9	118	*	82.8
APM – $V_T = 5$ mm/min	282.2	271.1	84	*	90.6
APM – $V_T = 20$ mm/min	333.8	293.6	54	*	139.7

By comparing Tables 3 and 4 it can be verified that the APM alloy tubing had higher strength. This is verified by the yield strength.

Figures 5a and 5b show the parametric Larson – Miller (L–M) curves summarizing data on creep rupture for the two alloys at a temperature range between 550° and 800°C. This temperature range was chosen due to the operational conditions which the steels were evaluated.



a) b)
Figure 5 – Parametric Curve of Larson & Miller, reuniting data... creep rupture for a) A268/Tp 446 and b) Alloy APM, in the range between 550°C and 800°C.

The A268 Tp/446 steel showed a creep resistance decrease with rupture life ranging between 500° and 700°C after the L–M analysis but, according to the regular standard expected, that is, with a trend to leveling Log (Stress) to small values of Log (Rupture Time). It should be noted that this methodology had difficulty to predicting results at 500° and 600°C at the lowest stress levels.

The APM steel showed a linear behavior of creep resistance decrease with a rupture life ranging between 500° and 800°C, which was unexpected. Larson – Miller’s parametric curves for each material (Figures 5a and 5b) provide an approach to the problem of predicting the lifecycle of these steels from the viewpoint of creep rupture.

The microstructural analysis was realized by optical microscopy. The A268/Tp 446 alloy presented a ferritic matrix and a primary lattice of carbides. The chemical composition and structure of carbides depend on the processing conditions and material composition. The formation of different types of carbides as a function of temperature and time. The precipitates in ferritic matrix are basically formed by $M_{23}C_6$ carbides \rightarrow $Cr_{23}C_6$ carbides. Certainly the microstructural changes observed in these sample are due exposure to temperature and stress at which was submitted. The powder metallurgy FeCrAl alloy APM by Kanthal alloy showed smaller amount of precipitates than A268/Tp 446 alloy. Figure 6 shows metallographic analysis a) A268/Tp 446 alloy and b) APM/kanthal alloy.

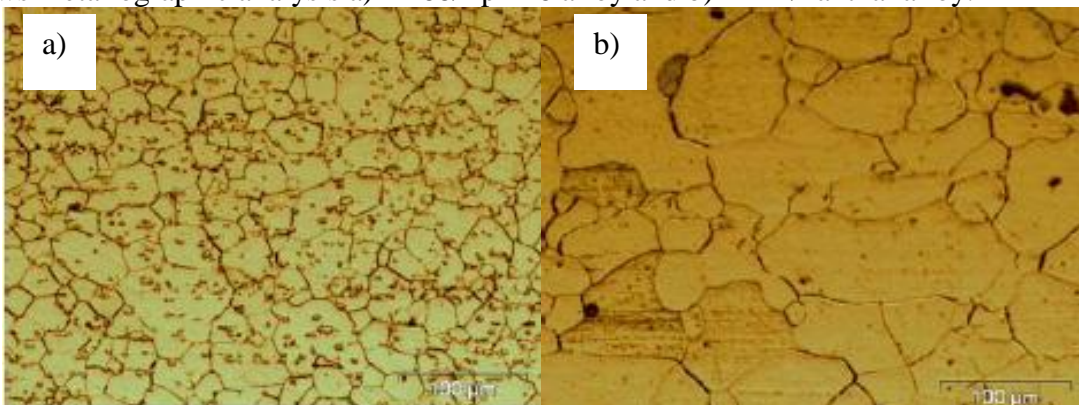


Figure 6 – Metallographic analysis a) A268/Tp 446 alloy and b) APM/kanthal alloy.

Figure 7a shows Scanning Electron Microscopy (SEM) of the A268/Tp 446 sample. It can be observed in these micrographs large amount of precipitates and a preferential corrosion. It was possible to identify occurrence of sigma phase (σ) with different geometries. These phases were confirmed by Energy Dispersive X-ray (EDX). The σ arises from the precipitation of chromium when the steel is maintained for a long time in isothermal levels (in the range of 500 - 800 °C). The APM/kanthal alloy presented smaller quantity of precipitates than A268/Tp 446 alloy according Figure 7a. A first instance is possible to conclude that APM/kanthal alloy is more resistant at high temperatures.

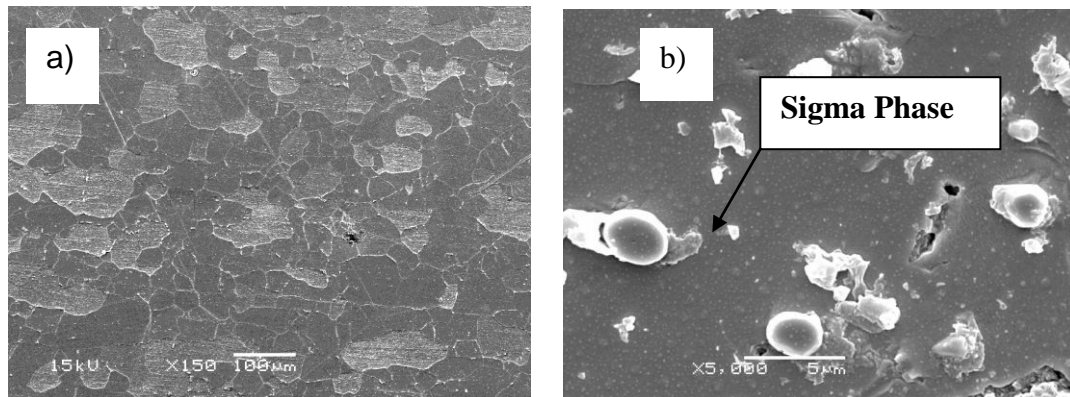


Figure 7 - SEM micrograph of the a) APM/kanthal alloy and b) A268/Tp 446 alloy.

Conclusions

This study assessed characteristics of ductility, tensile strength, yield strength, toughness and creep for two ferritic alloys: A268/Tp 446 and APM. Hot tensile tests and creep tests proved confirmed that APM is superior to A268/Tp 446 for short and long testing times. The set of parametric curves obtained through Larson- Miller for each material provided an approach to the problem of predicting the lifecycle of these steels from the viewpoint of creep rupture.

Acknowledgments

The authors would like to thank Petrobras/Un-Six, Laboratório de Eletroquímica de Superfície e Corrosão – LESC, Universidade Federal do Paraná – UFPR, Universidade Federal de São Carlos – UFSCar for support.

Bibliographic reference

- [1] GUEST, J.C. Standards in elevated temperature tensile and uniaxial creep testing. Proceedings of Conf. at Nat.Phys. Lab. p. 23-30. June 1981.
- [2] American Society for Testing and Materials. ASTM E – 21 – 79 (re-approved 1988), Annual Book of ASTM Standards (1988), pp. 190 – 196
- [3] BUENO, L.O. Creep Behaviour of 2.25Cr-1Mo steel – An equivalence between hot tensile and creep testing data. Proc. ECCO Creep Conf., 12-14 Sept.2006, London, Ed.by I.A.Shibli, S.R.Holdsworth,G.Merckling, DEStech Pub.Inc, 2005.
- [4] American Society for Testing and Materials, *Surface Engineering* (1996).
- [5] GITTUS, J. Creep, Viscoelasticity and creep rupture in solids, Applied Science Publishers, London, 1975.

- [7] BUENO, L.O., Proceedings of the II ETUAN / ABM – Anais do II Encontro de Tecnologia e Utilização dos Aços Nacionais, Rio de Janeiro (RJ), Brazil, p.916-934, 1987.
- [8] CONTIN JR, A. Comportamento de Fluência do Aço Inoxidável AISI 310 a 700°C – Uma Análise baseada no modelo de Tensão de Fricção. Dissertação de Mestrado Universidade Federal São Carlos, 1986.
- [9] DIETER, G.E. Mechanical Metallurgy, Third Edition, McGraw-Hill Book Company, London, p.289, 1988.